ARTICLE

Block Copolymer Assembly on Nanoscale Patterns of Polymer Brushes Formed by Electrohydrodynamic Jet Printing

M. Serdar Onses,[†,∥,#] Abelardo Ramírez-Hernández,[‡,§,#] Su-Mi Hur,[‡,§,#] Erick Sutanto,[⊥] Lance Williamson,[‡,§] Andrew G. Alleyne,[⊥] Paul F. Nealey,[‡,§] Juan J. de Pablo,[‡,§] and John A. Rogers[†,⊥,*]

[†]Department of Materials Science and Engineering, Beckman Institute, and Frederick Seitz Materials Research Laboratory, University of Illinois at Urbana-Champaign, Urbana, Illinois 61801, United States, [‡]Institute for Molecular Engineering, The University of Chicago, Chicago, Illinois 60637, United States, [§]Materials Science Division, Argonne National Laboratory, 9700 South Cass Avenue, Argonne, Illinois 60439, United States, [⊥]Department of Mechanical Science and Engineering, University of Illinois at Urbana-Champaign, Urbana, Illinois 61801, United States, and [∥]Department of Materials Science and Engineering, Erciyes University, Kayseri 38039, Turkey. [#]These authors contributed equally to this work.

ABSTRACT Fundamental understanding of the self-assembly of domains in block copolymers (BCPs) and capabilities in control of these processes are important for their use as nanoscale templates in various applications. This paper focuses on the self-assembly of spin-cast and printed poly(styrene-*block*-methyl methacrylate) BCPs on patterned surface wetting layers formed by electrohydrodynamic jet printing of random copolymer brushes. Here, end-grafted brushes that present groups of styrene and methyl methacrylate in geometries with nanoscale resolution deterministically define the morphologies of BCP nanostructures. The materials and methods can also be integrated with lithographically defined templates for directed self-assembly of BCPs at multiple length scales. The results provide not only engineering routes to controlled formation of complex patterns but also vehicles for experimental and simulation studies of the effects of chemical transitions on the processes of self-assembly. In particular, we show that the methodology developed here provides the means to explore exotic phenomena displayed by the wetting behavior of BCPs, where 3-D soft confinement, chain elasticity, interfacial energies, and substrate's surface energy cooperate to yield nonclassical wetting behavior.

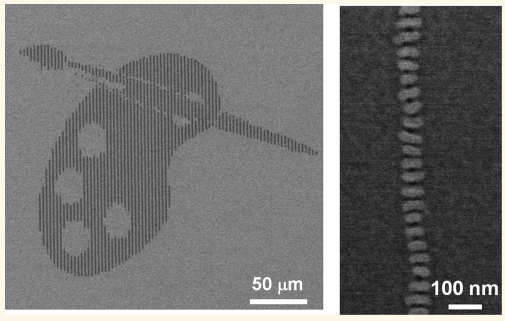

KEYWORDS: block copolymers · electrohydrodynamic jet printing · nanofabrication · polymer brushes · simulation

Block copolymers (BCPs) can self-assemble to form dense, nanoscale patterns as templates for applications in nanolithography,[1−3] membrane technology,[4] electronic devices,[5,6] and metamaterials.[7] Interfacial interactions determine the orientations of the domains that result from this type of assembly when it occurs in thin film geometries. For lithographic applications, nanoscale domains with orientations perpendicular to the substrate surface can serve as resists for the transfer of patterns to the underlying substrate. A well-established approach to engineer the proper orientation involves control of the wetting behavior of the substrate through surface grafting of random copolymer brushes that include monomers present in the BCP.[8,9] The composition of the brushes defines either preferential or non-preferential interactions with the blocks of the copolymer.[10] The latter leads to assembly of domains with orientations perpendicular to the substrate. Surfaces also play critical roles in the directed self-assembly (DSA) of BCPs, where topographically or chemically patterned substrates exert significant influence on the morphologies of the nanoscale domains.[11,12] In both cases, deposition of wetting layers typically involves spin-casting, to form uniform, unpatterned coatings. Most applications of BCPs demand fine spatial control of surface interactions across length scales that range from tens of nanometers to centimeters. Conventional lithographic techniques can be used to remove[13] uniform brush coatings in regions not protected by a resist or to define patterns of cross-linked polymer mats to prevent[14,15] brush grafting in selected regions. These methods require, however, multiple process steps and sacrificial layers that can cause difficulties in forming pristine surfaces or patterns that

* Address correspondence to jrogers@illinois.edu.

Received for review April 24, 2014 and accepted June 1, 2014.

Published online June 01, 2014
10.1021/nn5022605

incorporate more than a single brush chemistry. These and other limitations motivate the development of alternative, or complementary, techniques. An ideal approach would offer purely additive operation, nanoscale resolution, large-area compatibility, and capacity to directly pattern materials in a way that preserves their chemistry and leaves unpatterned surfaces in a completely unmodified state. Such capabilities are important not only for developing advanced methods in BCP-based nanofabrication, but also for fabricating test structures in fundamental studies of self-assembly.

Here, we report an additive scheme that uses electrohydrodynamically induced flows of liquids through fine nozzle tips to pattern well-defined surface wetting layers. The method, sometimes referred to as e-jet printing,[16] enables directed delivery of end-functional random copolymers with different compositions of styrene and methyl methacrylate, P(S-*ran*-MMA), to target surfaces in well-defined layouts. The resulting patterns dictate self-assembly processes in BCPs of poly(styrene-*block*-methyl methacrylate) (PS-*b*-PMMA). The additive nature of e-jet printing defines pristine chemical surfaces, in arbitrary geometries at length scales (~100 nm) sufficiently small to induce highly aligned arrays of self-assembled nanoscale domains. Even though it is possible to generate such nanoscale chemical patterns of polymer brushes with electron beam lithography, e-jet printing offers three unique and useful capabilities for control of phase behavior in BCPs. First, the purely additive operation preserves the chemistry of the printed materials and leaves unpatterned surfaces in a completely unmodified, pristine state. As a result, multiple brush chemistries can be exploited on a single substrate. Second, the jetting process allows delivery of brushes onto lithographically defined templates with significant surface topography, with important consequences in DSA. Third, the method offers options in combined patterning of brushes and BCPs,[17] as routes to engineered assemblies with unusual morphologies, chemistries and sizes on a single substrate.

RESULTS AND DISCUSSION

Figure 1a,b summarizes steps for patterning random copolymer brushes by e-jet printing. Applying a voltage between a metal coated glass capillary nozzle (1 μm internal diameter) and a freshly cleaned silicon wafer initiates controlled, pulsatile flow of inks that consist of P(S-*ran*-MMA) dissolved in an organic solvent through the nozzle tip. Movement of the stage[18] relative to the nozzle yields patterns of brushes in user-defined layouts. A brief thermal annealing step initiates surface condensation reactions between the hydroxyl terminus of the polymer and the silanol groups of the substrate. Washing away the unreacted material leaves covalently bound polymer brushes (Figure 1b). Height profiles of printed lines evaluated after each step (Supporting Information Figure S1) offer insights. The example here involves a line with a width of ~1 μm and a thickness of ~50 nm at the center. Thermal annealing results in a slight increase of the width and decrease in the height at the center of the line, likely due to thermally induced flow. Limiting the total amount of the printed material suppresses these flows (Supporting Information Figure S2) and also provides an additional means to control the width (Supporting Information Figure S3). The minimal degree of spreading can be reduced even further through optimization of the annealing conditions. Removing the ungrafted materials by sonication yields patterned brushes with uniform thicknesses of ~10 nm. The effects of annealing and washing can also be observed in discrete geometries such as squares (Supporting Information Figure S4). The functionality of the brushes can be assessed using spin-cast and thermally annealed films of a lamellae-forming BCP. Results indicate that the domains form with orientations perpendicular to the substrate in regions of printed P(S-*ran*-MMA) (62% S and 38% M, 62S), as shown in Figure 1c. The featureless regions in the unpatterned areas imply parallel assembly, in a stacked configuration with poly(methyl methacrylate) facing the surface of the substrate.

Diverse pattern geometries are possible, as illustrated in Figure 1d–f. Complex layouts (Figure 1d) can be defined using computer numerical control commands (*e.g.*, G-code) generated directly from an image (*e.g.*, jpeg) of the desired pattern. Advanced setups enable patterns in arbitrary curvilinear forms, as demonstrated by a series of concentric circular lines (Figure 1e). The radius of curvature can be sufficiently small (*e.g.* 1 μm) to observe perpendicular orientation of BCP domains in the curved regions, within the limits of our imaging techniques. The brushes can also be designed in the form of filled polygons with sharp edges, as shown in Figure 1f. The extreme uniformity in thickness and the low surface roughness (<0.5 nm) follow from the molecular processes and surface chemical bonding that define the height, as well as the high level of control in materials delivery provided by the e-jet approach. The influence of these features on the self-assembly of BCPs can be observed by spin coating a film of cylinder forming PS-*b*-PMMA (46-*b*-21 kg/mol) on top of the patterned substrate. Thermal annealing leads to island-hole structures in the unprinted regions (Figure 1g) as a result of the incommensurate thickness of the film with respect to the bulk periodicity of the BCP.[19] The grafted brush changes the wetting behavior from preferential to nonpreferential, thereby preventing the formation of such structures and instead forcing perpendicular assembly of BCP domains.

The ability to generate patterned surface polymer interactions at length scales that approach the sizes

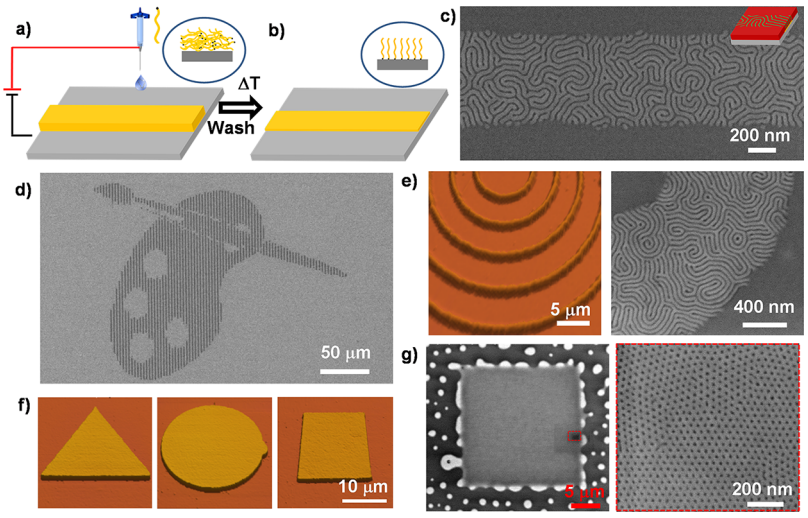

Figure 1. Versatility in patterning of random copolymer brushes using e-jet printing. (a and b) Schematic description of the process. The insets illustrate the arrangement of individual polymer chains in the printed brushes. (a) A voltage applied between a metal-coated glass nozzle and a silicon substrate with a native oxide layer initiates electrohydrodynamic flow and printing of inks that consist of hydroxyl-terminated P(S-*ran*-MMA) brushes with different compositions. (b) Thermal annealing at 220 °C for 5 min leads to grafting of the brushes to the substrate surface. Removal of excess unreacted material *via* repeated sonication in toluene leaves a pattern of brushes that are covalently bounded to the substrate. (c) SEM image of a self-assembled film of PS-*b*-PMMA (37-*b*-37) in a region that contains a printed line of the P(S-*ran*-MMA) brush. The inset provides an angled view illustration of the structure. (d) SEM image of a representative, complex pattern that can be achieved, with excellent uniformity over large areas. (e) Curvilinear features printed with P(S-*ran*-MMA) (62S). The AFM image on the left shows a series of concentric circular lines of the grafted brush (the height is ~10 nm). The SEM image on the right shows a self-assembled film of PS-*b*-PMMA (37-*b*-37) in a curved linear section of the patterned brush. (f) AFM images of grafted brushes that show the ability to print P(S-*ran*-MMA) in the form of filled pads with different geometries and consistent heights (~10 nm). (g) SEM image of a self-assembled film of a cylinder forming PS-*b*-PMMA (46-*b*-21) on a printed square of P(S-*ran*-MMA) (62S). A magnified SEM image is given on the right.

of individual domains allows direct influence on the self-assembly processes. Previous work[20,21] establishes that nanoscale chemical patterns can induce alignment of BCP domains in registration with the underlying patterns. To realize the necessary dimensions, we implemented an advanced form of e-jet printing in which fibrous polymer structures, rather than isolated droplets, emerge from the nozzle. This regime of operation, which can be considered as a "near field" type of electrospinning,[22] can yield aligned structures when implemented with fast motion of the substrate. Recent work demonstrates related methods for materials other than brushes.[23,24] This approach yields arrays of nanoscale lines of P(S-*ran*-MMA) with dimensions that are much smaller than the size of the nozzle (Figure 2a). The resulting chemical patterns provide controlled polymer surface interactions for perpendicular assembly of PS-*b*-PMMA domains (Figure 2b). The size of nozzle, concentration of the P(S-*ran*-MMA) in the ink and the printing parameters (*e.g.*, voltage and working distance) can be varied to allow patterns of brushes with sub-100 nm dimensions, as shown in Figure 2c. The smallest line widths (~50 nm) are a couple of times larger than the periodicity of the phase separated structures in the BCP. The resolution demonstrated here does not represent a fundamental limit. Optimizing the nozzle geometries, the accuracy of the electro-mechanical systems and the properties of the inks could lead to improvements.

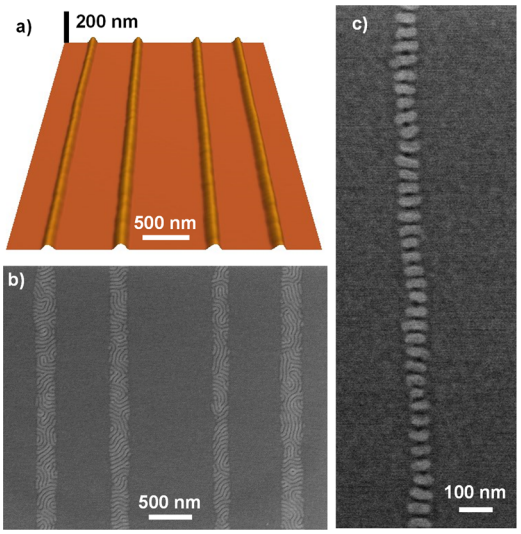

Figure 2. High resolution lines of random copolymer brushes formed by e-jet printing, operated in a near-field electrospinning mode. (a) AFM image of an array of printed lines of P(S-*ran*-MMA) (62S). (b and c) SEM image of a self-assembled PS-*b*-PMMA (37-*b*-37) film cast on top of these brushes. The result illustrates a remarkable level of alignment in the nanoscale domains.

Here, highly aligned nanoscale domains form along the entire lengths of the lines and fully across their widths. Related self-alignment effects, over much smaller areas, are possible in chemical patterns formed by electron beam lithography, as reported by Shin *et al.*[25]

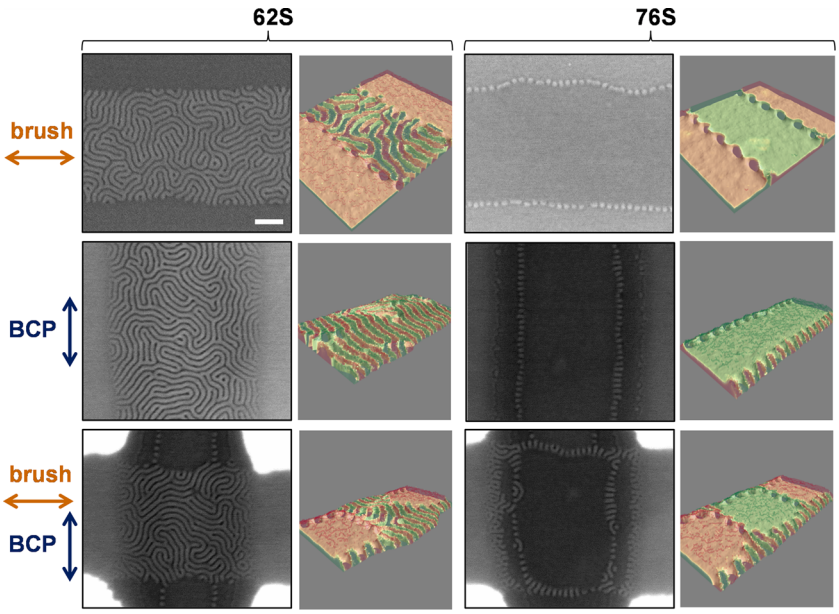

Figure 3. BCP self-assembly near regions of chemical transitions provided by patterns of random copolymer brushes formed by e-jet printing. SEM (on the left) and corresponding 3-D simulation images (on the right) for two different brush compositions (62S and 76S). Row 1: a spin-cast film (~35 nm) of PS-*b*-PMMA (37-*b*-37) assembled on top of the patterned brushes in a horizontal stripe geometry. Row 2: a printed line of PS-*b*-PMMA (37-*b*-37) assembled on top of the homogeneous brush grafted region. Row 3: a printed line of PS-*b*-PMMA (37-*b*-37) assembled on top of the patterned brushes in a horizontal stripe geometry. The thickness of the printed BCP line at the center is ~40 nm. The scale bar is 200 nm for the SEM images. The PS and PMMA blocks are represented with red and green color in the simulation images, respectively.

Brushes delivered to surfaces by e-jet printing yield sharp interfaces, with abrupt transitions in the chemistry of the substrate surface. The result induces assembly of BCPs into unique nanoscale morphologies near the edges of the patterned features. Systematic experimental and simulation studies illuminate the effects on the assembly of lamellae forming PS-*b*-PMMA BCPs spin-cast and printed on top of patterned stripes of brushes on a silicon substrate (Figure 3). The investigations exploit two types of P(S-*ran*-MMA) brushes, for nonpreferential (62S) and PS preferential (76S) interactions. Monte Carlo simulations using a coarse grain model for copolymers with a molecular representation[26] capture the behaviors (see Supporting Information for details of the model and simulation approach).

The first case involves the assembly of a film of PS-*b*-PMMA spin-cast on top of printed brushes (Figure 3, row 1). Domains assemble parallel to the substrate in the unpatterned regions due to the strongly preferential interactions of the PMMA block with the silicon. By contrast, on 62S, domains assemble in perpendicular orientations across the entire printed region, with almost equal presence of PS and PMMA domains near the edges (see more images in Supporting Information Figure S3). The arrangement of domains predicted by simulations agrees well with the experiments (for top-view simulation images see Supporting Information Figure S5). The copolymer grains on and near the patterned brushes meet at the edge and configure themselves in a manner that minimizes interfacial area. In this case, the geometry satisfies Scherk's first minimal surface.[27−29] Therefore, perpendicular domains tend to also align perpendicular to the edge, which explains the equal presence of PS and PMMA domains. Thus, the creation of this minimal surface breaks the rotational symmetry in the plane and a preferred orientation is selected, which should induce the formation of well aligned perpendicular lamellae along the axis of the printed brush line. Defects, however, frustrate realization of this perfect morphology. Decreasing the width of the nonpreferential region diminishes the role of such defects, thereby improving the alignment, as shown in Figure 2. On 76S (Figure 3, row 1), PS preferential interactions lead to lamellae with parallel orientation, except the edges where the domains appear to assemble perpendicular to the substrate with an interesting one-dimensional arrangement. The simulations accurately predict these results and also capture the full three-dimensional structure of the BCP film, where perpendicular features are found to localize at the near of the top interface of the film. This behavior is a consequence of screw dislocations that arise from the shift between parallel layers at the edge, and the chain connectivity that yields a periodicity in those features along the edge.[30] In both brush compositions (62S and 76S), the generation of boundaries between "grains" leads to continuous polymer domains.

Departing from the classical spin-casted BCP films, the use of e-jet printing[17] to deposit BCPs in a linear

geometry leads to additional types of morphologies on and near the patterned brushes (Figure 3, row 2 and 3). The orientation of domains is perpendicular through the printed line on patterned 62S, as observed with spin-coated BCP films. On the other hand, mixed types of morphologies appear near the edges for the PS preferential (76S) brush patterns. A narrow terrace like region is also present near the edges for the printed BCP on preferential wetting substrates as reported previously.[17] These types of morphologies are likely to result from abrupt changes in the chemistry of the brushes as well as variations in thickness along the width of the printed BCP line. Thickness is known to be important in the assembly of BCPs on weakly preferential substrates.[19,31] The importance of the thickness in such 3-D films is further supported by the observation of different morphologies across the width of BCP nanostructures deposited with an AFM tip.[32] Additionally, thickness gradients across the width of the printed BCP lines may also play a role in the determination of morphologies, as previously[33,34] demonstrated through self-alignment of lamellar domains in the direction of the thickness modulation in PS-*b*-PMMA films patterned by evaporation driven self-assembly. The lack of such alignment effects in our system could be due to the significantly smaller line widths and thicknesses compared to those of previous work.

The simulations indicate that surface energies play a key role in the morphologies of printed BCPs on and near the printed brushes. Contrary to typical DSA studies where the surface energies of the substrate and the BCP material (in case of blocks with similar surface tension) are not relevant to the process, here they are crucial in defining the equilibrium morphology. The interplay of 3-D soft confinement, configurational chain entropy and, interfacial and surface energies can result in the selection of a specific orientation (self-alignment) or in more complex morphologies unexpected from the BCP phase diagram in the bulk. The high surface energies associated with both the substrate and the BCP lead to a very low contact angles for the BCP. Simulation results (Figure 3, row 2) for a line of BCP printed on a homogeneous brush agree with the experimental observations. On 62S, the domains assemble perpendicular to the substrate over the entire printed BCP line. Furthermore, the low contact angle of the BCP line leads to preferential alignment with the interface of BCP domains perpendicular to the edge, but defects prevent the formation of long-range order. This breaking of symmetry arises from the balance of the factors mentioned above; in particular, under low contact angle constraint, other chain orientations involve bending of interfaces and/or chain stretching, none being compensated by other terms in the free energy, therefore yielding nonstable configurations. On 76S, domains orient parallel to the substrate in the central regions of the BCP line. This orientation is unfavorable, however, near the edges due to the large chain stretching and entropic penalties that result. The domains therefore prefer to orient perpendicular to the substrate at the edge in spite of an enthalpic cost. For BCP lines printed on patterned stripes of brushes (Figure 3, row 3), the BCP interacts with both the bare substrate (PMMA preferential) and the nonpreferential or PS preferential regions. The SEM images show that the domains orient parallel to the bare substrate with perpendicular domains at the edges due to the low contact angle of the BCP. On top of the nonpreferential brush, the orientation of domains is similar to that of the BCP line printed onto a substrate with a homogeneous brush. On the PS-preferential brush stripe, the low contact angle constraint and the screw dislocations at the "grain boundary" produce a series of perpendicular decorations along the edges. While the simulations capture the main features of the printed BCPs on a preferential substrate, they are unable to reproduce the apparent narrow terrace-like region observed in the experiments, presumably due to limitations in the size in simulations and the difficulties in reproducing high surface energy values in our modeling approach.

E-jet printed BCPs with cylindrical morphology reveal unique features including self-alignment effects on and near printed patterns of brushes. The asymmetric composition of a cylinder forming PS-*b*-PMMA (46-*b*-21) leads to an interesting arrangement of domains near the edges of the printed BCPs and brushes. While perpendicularly oriented cylinders occur along the printed BCPs on a nonpreferential brush (Figure 4a), mixed (parallel and perpendicular cylinders) morphologies appear on and near the edges of PS or PMMA preferential regions (see images in Supporting Information Figure S6). Simulation results (Supporting Information Figure 7) suggest that the thickness plays an important role on the printed cylinder forming BCPs: in particular, a transition from parallel to perpendicular occurs as the thickness increases. A particularly interesting effect observed in many cases is self-alignment of the domains parallel to the long axis of the printed BCP line on the PMMA preferential wetting bare Si substrate (Figure 4b). When these domains approach a patterned stripe of a nonpreferential brush, the direction of alignment changes from parallel to perpendicular with respect to the long axis of the printed BCP line (Figure 4c,d). On the other hand, the orientation of domains with respect to the substrate switches from parallel to perpendicular in the region of the brush. Simulations indicate that the alignment of parallel cylinders close to the region of the nonpreferential brush is induced by the grain of perpendicular cylinders (Supporting Information Figure 8). This result provides an example of the unprecedented control of

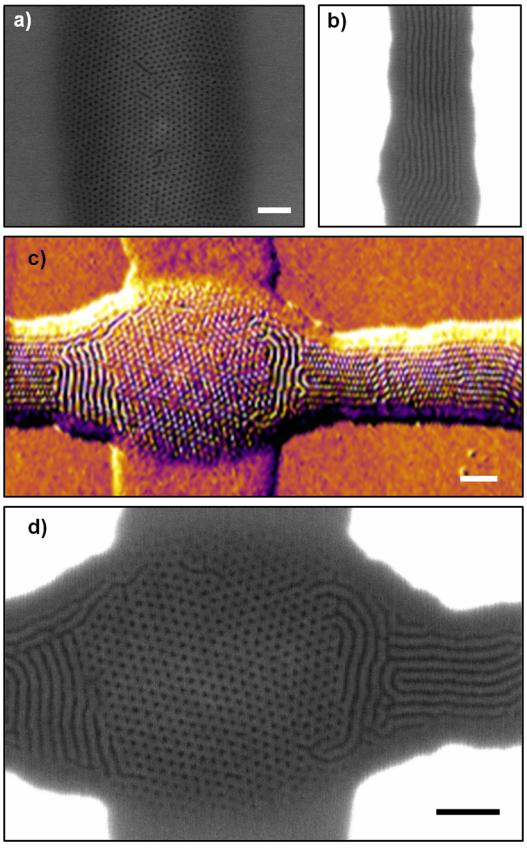

Figure 4. Self-alignment of printed patterns of a cylinder forming BCP on and near printed patterns of brushes. SEM image of the assembled cylinder forming PS-*b*-PMMA (46-*b*-21) on top of the (a) brush (62S) grafted region and (b) a silicon substrate with a native oxide layer. (c) AFM and (d) SEM image of the assembled, printed BCP film near brushes (62S) patterned in a vertical stripe geometry. The scale bar in the images is 200 nm.

domain arrangement in and out of the plane, uniquely enabled by combined patterning of both the brushes and BCPs by e-jet printing. The thickness uniformity of the printed BCP films can help to ensure uniformity in patterns transferred *via* use of these films as resists. Printing BCPs in the form of filled pads with a high level of uniformity (roughness <2 nm) as shown previously[17] and using lithographically defined trenches, filled with BCPs *via* e-jet printing can provide the necessary uniformity in thickness. BCPs with high etch selectivity or with subsequently hardened blocks can further enhance this uniformity.

Combining printed brushes with substrates that support predefined, lithographic structures[35] affords additional levels of control. In the example presented in Figure 5, features of hydrogen silsesquioxane (HSQ) defined by electron beam lithography on a silicon substrate yield topographical features with chemically homogeneous surfaces. Functionalization of selected trenches (bottoms and sidewalls) with P(S-*ran*-MMA) by e-jet printing yields spatial control over the chemistry of these features (Figure 5a). This chemical contrast yields distinct wetting behaviors and assembly of

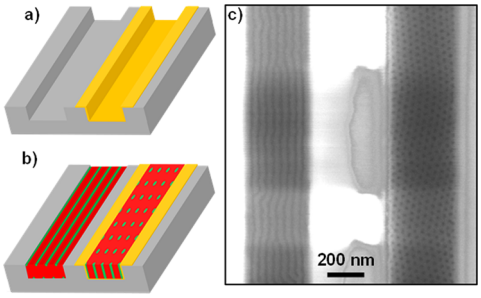

Figure 5. Spatial control over the morphology of nanoscale domains in BCPs formed on substrates that combine topographical patterns with printed brushes. (a and b) Schematic illustration of the experiment. (a) Aligned printing and grafting of P(S-*ran*-MMA) (62S) on selected trenches separately fabricated by electron beam lithography. (b) Assembly of a film of a cylinder forming PS-*b*-PMMA (46-*b*-21) spin-cast on trenches with printed brushes. (c) SEM image of the assembled BCP film that shows parallel and perpendicular orientation of the domains within the trenches without and with brushes, respectively.

a cylinder forming PS-*b*-PMMA on adjacent trenches (Figure 5b,c). On the bare trench (left), cylinders lie parallel to the substrate surface, with a high level of in-plane alignment along the axis of the template. The neutral wetting behavior of the trench (right) functionalized with the brush leads to guided assembly of cylinders oriented perpendicular to the substrate. Previous work[31] demonstrates that the thickness of the BCP film is critically important to achieving a high level of in-plane alignment of the perpendicularly oriented domains within trenches that have same wetting behaviors on the bottom and sidewalls. These printing approaches can easily be adapted for DSA of BCP films that exploit chemical, rather than topographical, patterns:[14] here, random copolymer brushes can be printed on top of the lithographically prepared templates to spatially define the one component of the binary chemical patterns.

CONCLUSIONS

The results presented here demonstrate several unique capabilities that follow from direct, high resolution electrohydrodynamic delivery of random copolymer brushes as surface wetting layers to control the geometries of nanoscale domains in spin-cast and printed BCPs. Here, patterns of brushes with complex geometries and feature sizes down to ~50 nm combine with natural processes of self-assembly to provide unusual options in patterning of surfaces at multiple length scales. Some of these sharp, chemically pristine patterns also reveal fundamental effects in BCP assembly, as illuminated by combined experimental and modeling studies. Other possibilities include the adaptation of these approaches in patterning of top-coat[36] materials on BCP films to provide neutral layers for perpendicular assembly of domains with sub-10 nm

dimensions. Developing ink compositions suitable for brushes with different chemistries of use in nanotechnology[37] and biotechnology[38] also appears promising for future work.

METHODS

Substrate, Nozzle, and Ink Preparation. Silicon wafers (⟨100⟩, WRS Materials) were cleaned using an oxygen plasma treatment (200 W, 200 mT, 20 sccm) for 5 min. Prepulled glass pipettes (World Precision Instruments) with inner nozzle diameters of 1 μm were coated (Denton, Desk II TSC) with Au/Pd by sputter deposition. The resulting metal coated nozzles were treated with a hydrophobic solution (0.1% perfluorodecanethiol in DMF) for 10 min and then dipped in DMF for 10 s and dried with air. A solution (0.1%−1%) of hydroxyl-terminated random copolymers in 1,2,4-trichlorobenzene (≥99%, Sigma-Aldrich) served as the ink. Random copolymers were synthesized following the procedures reported in the previous study[10] with styrene and methyl methacrylate compositions of 57%:43% (57S, ∼3 kg/mol), 62%:38% (62S, ∼12 kg/mol), and 76%:24% (76S, ∼10 kg/mol).

Electrohydrodynamic Jet Printing of Brushes. A voltage (350-450 V) was applied between a metal-coated glass capillary and a grounded substrate with a standoff height of ∼30 μm. For the results presented in Figure 2, the voltage was chosen ∼25 V higher than the minimum voltage (250−300 V depending on the printing conditions) required to initiate printing. Spatial control of the printing process was provided by a 5-axis stage interfaced to a computer for coordinated control of voltage applied to the nozzle.

Processing of Printed Brushes. The patterned substrate was annealed at 220 °C for 5 min in a glovebox filled with nitrogen. After annealing, ungrafted polymers were removed by 3 cycles of sonication in warm toluene for 3 min per cycle and then dried with nitrogen. A film of BCP (37-37 and 46-21 kg/mol, Polymer Source, Inc.) was then either spin-coated (Toluene) or printed (1,2,4-trichlorobenzene).

Characterization of Polymer Brushes and BCP Film Morphologies. The surface morphologies were imaged with a field emission scanning electron microscope (SEM, Hitachi S-4800) at 1 kV. The topographies of the printed polymer brushes and the BCP films were analyzed with an AFM (Asylum Research MFP-3D) in tapping mode using a silicon tip with aluminum reflex coating (Budget Sensors).

Conflict of Interest: The authors declare no competing financial interest.

Supporting Information Available: Details of the simulation methods, additional AFM and SEM characterization of the printed brushes, experimental and simulation results of BCPs spin-cast and printed on patterned brushes. This material is available free of charge *via* the Internet at http://pubs.acs.org.

Acknowledgment. This work was supported by the Center for Nanoscale Chemical Electrical Mechanical Manufacturing Systems at the University of Illinois (funded by the National Science Foundation under Grant CMMI-0749028) and Air Force Office of Scientific Research MURI FA9550-12-1-0471. We gratefully acknowledge the computing resources provided on Blues, high-performance computing cluster operated by the Laboratory Computing Resource Center at Argonne National Laboratory. A.R.H., S.M.H., P.F.N. and J.J.d.P. acknowledge support from U.S. Department of Energy, Office of Science, Office of Basic Energy Sciences-Materials Science, under contract DE-AC02-06CH11357. AFM and SEM studies were carried out in the Frederick Seitz Materials Research Laboratory Central Facilities, University of Illinois.

REFERENCES AND NOTES

1. Ruiz, R.; Kang, H. M.; Detcheverry, F. A.; Dobisz, E.; Kercher, D. S.; Albrecht, T. R.; de Pablo, J. J.; Nealey, P. F. Density Multiplication and Improved Lithography by Directed Block Copolymer Assembly. *Science* **2008**, *321*, 936–939.
2. Kim, B. H.; Kim, J. Y.; Kim, S. O. Directed Self-Assembly of Block Copolymers for Universal Nanopatterning. *Soft Matter* **2013**, *9*, 2780–2786.
3. Park, M.; Harrison, C.; Chaikin, P. M.; Register, R. A.; Adamson, D. H. Block Copolymer Lithography: Periodic Arrays of Similar to 10(11) Holes in 1 Square Centimeter. *Science* **1997**, *276*, 1401–1404.
4. Yin, J.; Yao, X. P.; Liou, J. Y.; Sun, W.; Sun, Y. S.; Wang, Y. Membranes with Highly Ordered Straight Nanopores by Selective Swelling of Fast Perpendicularly Aligned Block Copolymers. *ACS Nano* **2013**, *7*, 9961–9974.
5. Black, C. T.; Guarini, K. W.; Milkove, K. R.; Baker, S. M.; Russell, T. P.; Tuominen, M. T. Integration of Self-Assembled Diblock Copolymers for Semiconductor Capacitor Fabrication. *Appl. Phys. Lett.* **2001**, *79*, 409–411.
6. Farrell, R. A.; Kinahan, N. T.; Hansel, S.; Stuen, K. O.; Petkov, N.; Shaw, M. T.; West, L. E.; Djara, V.; Dunne, R. J.; Varona; et al. Large-Scale Parallel Arrays of Silicon Nanowires *via* Block Copolymer Directed Self-Assembly. *Nanoscale* **2012**, *4*, 3228–3236.
7. Vignolini, S.; Yufa, N. A.; Cunha, P. S.; Guldin, S.; Rushkin, I.; Stefik, M.; Hur, K.; Wiesner, U.; Baumberg, J. J.; Steiner, U. A 3D Optical Metamaterial Made by Self-Assembly. *Adv. Mater.* **2012**, *24*, Op23–Op27.
8. Mansky, P.; Liu, Y.; Huang, E.; Russell, T. P.; Hawker, C. J. Controlling Polymer-Surface Interactions with Random Copolymer Brushes. *Science* **1997**, *275*, 1458–1460.
9. Ryu, D. Y.; Shin, K.; Drockenmuller, E.; Hawker, C. J.; Russell, T. P. A Generalized Approach to the Modification of Solid Surfaces. *Science* **2005**, *308*, 236–239.
10. Han, E.; Stuen, K. O.; La, Y. H.; Nealey, P. F.; Gopalan, P. Effect of Composition of Substrate-Modifying Random Copolymers on the Orientation of Symmetric and Asymmetric Diblock Copolymer Domains. *Macromolecules* **2008**, 9090–9097.
11. Tavakkoli, K. G. A.; Gotrik, K. W.; Hannon, A. F.; Alexander-Katz, A.; Ross, C. A.; Berggren, K. K. Templating Three-Dimensional Self-Assembled Structures in Bilayer Block Copolymer Films. *Science* **2012**, *336*, 1294–1298.
12. Liu, C. C.; Ramirez-Hernandez, A.; Han, E.; Craig, G. S. W.; Tada, Y.; Yoshida, H.; Kang, H. M.; Ji, S. X.; Gopalan, P.; de Pablo, J. J.; *et al.* Chemical Patterns for Directed Self-Assembly of Lamellae-Forming Block Copolymers with Density Multiplication of Features. *Macromolecules* **2013**, *46*, 1415–1424.
13. Stoykovich, M. P.; Muller, M.; Kim, S. O.; Solak, H. H.; Edwards, E. W.; de Pablo, J. J.; Nealey, P. F. Directed Assembly of Block Copolymer Blends into Nonregular Device-Oriented Structures. *Science* **2005**, *308*, 1442–1446.
14. Liu, C. C.; Han, E.; Onses, M. S.; Thode, C. J.; Ji, S. X.; Gopalan, P.; Nealey, P. F. Fabrication of Lithographically Defined Chemically Patterned Polymer Brushes and Mats. *Macromolecules* **2011**, *44*, 1876–1885.
15. Onses, M. S.; Liu, C. C.; Thode, C. J.; Nealey, P. F. Highly Selective Immobilization of Au Nanoparticles onto Isolated and Dense Nanopatterns of Poly(2-vinyl pyridine) Brushes down to Single-Particle Resolution. *Langmuir* **2012**, *28*, 7299–7307.
16. Park, J. U.; Hardy, M.; Kang, S. J.; Barton, K.; Adair, K.; Mukhopadhyay, D. K.; Lee, C. Y.; Strano, M. S.; Alleyne, A. G.; Georgiadis, J. G.; *et al.* High-Resolution Electrohydrodynamic Jet Printing. *Nat. Mater.* **2007**, *6*, 782–789.
17. Onses, M. S.; Song, C.; Williamson, L.; Sutanto, E.; Ferreira, P. M.; Alleyne, A. G.; Nealey, P. F.; Ahn, H.; Rogers, J. A. Hierarchical Patterns of Three-Dimensional Block-Copolymer Films Formed by Electrohydrodynamic Jet Printing and Self-Assembly. *Nat. Nanotechnol.* **2013**, *8*, 667–675.

18. Sutanto, E.; Shigeta, K.; Kim, Y. K.; Graf, P. G.; Hoelzle, D. J.; Barton, K. L.; Alleyne, A. G.; Ferreira, P. M.; Rogers, J. A. A Multimaterial Electrohydrodynamic Jet (E-jet) Printing System. *J. Micromech. Microeng.* **2012**, *22*, 1–11.
19. Suh, H. S.; Kang, H. M.; Nealey, P. F.; Char, K. Thickness Dependence of Neutral Parameter Windows for Perpendicularly Oriented Block Copolymer Thin Films. *Macromolecules* **2010**, *43*, 4744–4751.
20. Rockford, L.; Liu, Y.; Mansky, P.; Russell, T. P.; Yoon, M.; Mochrie, S. G. J. Polymers on Nanoperiodic, Heterogeneous Surfaces. *Phys. Rev. Lett.* **1999**, *82*, 2602–2605.
21. Kim, S. O.; Solak, H. H.; Stoykovich, M. P.; Ferrier, N. J.; de Pablo, J. J.; Nealey, P. F. Epitaxial Self-Assembly of Block Copolymers on Lithographically Defined Nanopatterned Substrates. *Nature* **2003**, *424*, 411–414.
22. Greiner, A.; Wendorff, J. H. Electrospinning: A Fascinating Method for the Preparation of Ultrathin Fibres. *Angew. Chem., Int. Ed.* **2007**, *46*, 5670–5703.
23. Min, S. Y.; Kim, T. S.; Kim, B. J.; Cho, H.; Noh, Y. Y.; Yang, H.; Cho, J. H.; Lee, T. W. Large-Scale Organic Nanowire Lithography and Electronics. *Nat. Commun.* **2013**, *4*, 1–9.
24. Huang, Y. A.; Bu, N. B.; Duan, Y. Q.; Pan, Y. Q.; Liu, H. M.; Yin, Z. P.; Xiong, Y. L. Electrohydrodynamic Direct-Writing. *Nanoscale* **2013**, *5*, 12007–12017.
25. Shin, D. O.; Kim, B. H.; Kang, J. H.; Jeong, S. J.; Park, S. H.; Lee, Y. H.; Kim, S. O. One-Dimensional Nanoassembly of Block Copolymers Tailored by Chemically Patterned Surfaces. *Macromolecules* **2009**, *42*, 1189–1193.
26. Detcheverry, F. A.; Kang, H. M.; Daoulas, K. C.; Muller, M.; Nealey, P. F.; de Pablo, J. J. Monte Carlo Simulations of a Coarse Grain Model for Block Copolymers and Nanocomposites. *Macromolecules* **2008**, *41*, 4989–5001.
27. Thomas, E. L.; Anderson, D. M.; Henkee, C. S.; Hoffman, D. Periodic Area-Minimizing Surfaces in Block Copolymers. *Nature* **1988**, *334*, 598–601.
28. Gido, S. P.; Gunther, J.; Thomas, E. L.; Hoffman, D. Lamellar Diblock Copolymer Grain-Boundary Morphology 0.1. Twist Boundary Characterization. *Macromolecules* **1993**, *26*, 4506–4520.
29. Liu, G. L.; Ramirez-Hernandez, A.; Yoshida, H.; Nygard, K.; Satapathy, D. K.; Bunk, O.; de Pablo, J. J.; Nealey, P. F. Morphology of Lamellae-Forming Block Copolymer Films between Two Orthogonal Chemically Nanopatterned Striped Surfaces. *Phys. Rev. Lett.* **2012**, 108.
30. Kamien, R. D.; Lubensky, T. C. Minimal Surfaces, Screw Dislocations, and Twist Grain Boundaries. *Phys. Rev. Lett.* **1999**, *82*, 2892–2895.
31. Kim, M.; Han, E.; Sweat, D. P.; Gopalan, P. Interplay of Surface Chemical Composition and Film Thickness on Graphoepitaxial Assembly of Asymmetric Block Copolymers. *Soft Matter* **2013**, *9*, 6135–6141.
32. Felts, J. R.; Onses, M. S.; Rogers, J. A.; King, W. P. Nanometer Scale Alignment of Block−Copolymer Domains by Means of a Scanning Probe Tip. *Adv. Mater.* **2014**, *26*, 2999–3002.
33. Kim, B. H.; Shin, D. O.; Jeong, S. J.; Koo, C. M.; Jeon, S. C.; Hwang, W. J.; Lee, S.; Lee, M. G.; Kim, S. O. Hierarchical Self−Assembly of Block Copolymers for Lithography−Free Nanopatterning. *Adv. Mater.* **2008**, *20*, 2303–2307.
34. Kim, B. H.; Lee, H. M.; Lee, J. H.; Son, S. W.; Jeong, S. J.; Lee, S.; Lee, D. I.; Kwak, S. U.; Jeong, H.; Shin, H. Spontaneous Lamellar Alignment in Thickness−Modulated Block Copolymer Films. *Adv. Funct. Mater.* **2009**, *19*, 2584–2591.
35. Luo, M.; Epps, T. H. Directed Block Copolymer Thin Film Self-Assembly: Emerging Trends in Nanopattern Fabrication. *Macromolecules* **2013**, *46*, 7567–7579.
36. Bates, C. M.; Seshimo, T.; Maher, M. J.; Durand, W. J.; Cushen, J. D.; Dean, L. M.; Blachut, G.; Ellison, C. J.; Willson, C. G. Polarity-Switching Top Coats Enable Orientation of Sub-10-nm Block Copolymer Domains. *Science* **2012**, *338*, 775–779.
37. Onses, M. S.; Nealey, P. F. Tunable Assembly of Gold Nanoparticles on Nanopatterned Poly(ethylene glycol) Brushes. *Small* **2013**, *9*, 4168–4174.
38. Hucknall, A.; Rangarajan, S.; Chilkoti, A. In Pursuit of Zero: Polymer Brushes that Resist the Adsorption of Proteins. *Adv. Mater.* **2009**, *21*, 2441–2446.